30
12/29/86 JS 3 Distb ㉗

J-29017

DR#0069-8

UCID--20934

DE87 003606

THE EFFECT OF TARGET THICKNESS ON X-RAY PRODUCTION BY FXR

Norman L. Back

October 22, 1986

Lawrence
Livermore
National
Laboratory

Work performed under the auspices of the U.S. Department of Energy by the Lawrence Livermore National Laboratory under Contract W-7405-Eng-48.

THE EFFECT OF TARGET THICKNESS ON X-RAY PRODUCTION BY FXR

Norman L. Back
October 22, 1986

ABSTRACT

The electron-photon transport code SANDYL has been used to calculate the x-ray flux for a simplified Flash X-Ray Machine (FXR) bullnose geometry. Four different thicknesses (24.5, 36.75, 49, and 61.25 mils) were used for the tantalum bremsstrahlung target in order to study the effect of target thickness on the FXR output. The calculations were performed for a parallel 17 MeV electron beam, and the resulting angular distributions were then used to compute the forward flux for the more realistic case of a converging beam. Over the range of thicknesses studied, the x-ray energy content per steradian on axis was essentially independent of target thickness. The main reason for this is that, while the total x-ray flux coming out of the target increases with increasing target thickness, the angular width of that flux also increases. The implications for target wheel design are discussed.

I. INTRODUCTION

A number of questions have been raised about the thickness of the tantalum targets that are used in the FXR to convert electron beam energy into x-ray flux. These questions are particularly important now, since a new type of target wheel has been designed which has a fixed uniform thickness of tantalum rather than holes into which tantalum coupons of arbitrary thickness can be inserted. One thing we need to know is whether 40 mils (the design thickness for the new wheel) is the correct value to use. Also, is the ±5 mil tolerance appropriate? What happens to the x-ray flux, spectrum, and angular distribution when we change the target thickness? Our past experience with 30 and 40 mil coupons, though inconclusive, did indicate that the target thickness may not be very important. Therefore, this computer study was undertaken to examine the problem over a wider range of thicknesses and to find out what physical effects are important in determining the relation between target thickness and x-ray flux.

II. GEOMETRY

Over the past year or so, a standard bullnose geometry has been developed for use in hydro shots. This geometry is quite complicated, and what I used for calculational purposes was only an approximation of it. However, for photons or electrons which originate at the center of the target, and travel in straight lines to the bullnose exit without hitting any of the heavy collimating material, the geometry shown in Fig. 1 is an accurate representation. The limiting ray in the real geometry, which is determined by the one inch diameter hole through the middle of the D-38 "donuts", makes an angle of 2.6° with the beam centerline. For a typical hydro shot, with the first film at 390 inches from the target, this limiting ray hits the film at 17.6 inches from the center, so the direct radiation just barely illuminates an entire 22 by 28 inch sheet of film. For the geometry of Fig. 1, the limiting angle is 2.4°.

Four different tantalum target thicknesses (24.5, 36.75, 49, and 61.25 mils) were used in these calculations. In each case, the nominal thickness was divided by cos 30° to account for the tilt of the target. In addition to the zones shown in Fig. 1, I defined some thin "edit" zones in order to sample the energy and angle dependence of the photon flux at five different locations. The edit zone that I concentrated on for the analysis described in this paper was the one immediately after the counterbored section of the beryllium beam stop (zone 10). The results for edit zones located further downstream are similar except for attenuation and spreading, both of which turned out to be independent of target thickness.

For the angular distribution studies described below, I used an even simpler geometry. It was the same as the geometry of Fig. 1, except that (a) it stopped at zone 10 and (b) the radius of both the inner and outer cylinders was increased to 2.75 cm. This allowed me to get an angular distribution at the location of zone 10 which was good out to 17°.

III. RESULTS

Figure 2 shows the spectrum of x-rays entering zone 10 at angles between 0 and 1°, for a 17 MeV parallel electron beam hitting the 36.75 mil target. The meanings of the various terms used in this figure are explained in detail in Ref. 1 (the methodology of which was used here to the maximum possible extent). The SANDYL (Ref. 2) calculation used to produce this spectrum required 214 minutes of CDC 7600 time to follow 200000 primary particles. The spectra obtained using target thicknesses of 24.5, 49, and 61.25 mils were very similar to this one both in shape and in magnitude. The total integrated photon yields obtained from these spectra are (for photon energies greater than 0.75 MeV):

Thickness(mils)	Photons/steradian/electron
24.5	3.22 ± 0.12
36.75	3.32 ± 0.12
49	3.12 ± 0.13
61.25	3.05 ± 0.12

Of course, photons of different energies are not equivalent for radiographic purposes, so the numbers given above are not particularly meaningful. Another, somewhat arbitrary, measure of the x-ray output is the total energy content, obtained by multiplying the number of photons in each energy bin by the average energy in that bin and then adding up all the contributions between 0.75 and 17 MeV. This procedure has the virtue of weighting more heavily the radiographically more important high-energy photons. The results are (for angles between 0 and 1°):

Thickness(mils)	Photon*MeV/steradian/electron
24.5	13.37 ± 0.69
36.75	14.65 ± 0.71
49	13.56 ± 0.76
61.25	12.53 ± 0.63

So it appears that both the total flux and the total energy content reach maxima at 36.75 mils and then decrease monotonically at greater thicknesses. This is not a firm conclusion, however, because of the large statistical errors. Indeed, there would be almost as much justification for saying that these two quantities are independent of thickness.

Note that everything up to this point was done for a parallel electron beam, even though the actual FXR beam is not parallel but instead converges to a small spot on the target. Nevertheless, according to Refs. 1 and 3, there is a simple procedure for deducing the photon flux on axis from a converging electron beam, if the beam is assumed to be uniformly distributed in solid angle inside a cone whose vertex is at the target center. This procedure is based on the fact that the flux per unit solid angle on axis produced by an electron converging at a given angle is approximately equal to the flux per unit solid angle at the equivalent photon angle produced by an axial electron. It is valid if the materials that the photons pass through are the same both on- and off-axis and if the angles involved are small enough that we can ignore the slight differences in electron and photon path lengths.

The first step in this procedure was to calculate the angular distribution of the photons for each target thickness. To do this, I reran SANDYL using the simplified geometry mentioned above, so that I could extend the angular distribution all the way out to 17°. Also, to save computer time, I reduced the number of primary particles in the calculation by a factor of 10. This, of course, increased the statistical errors by a factor of 3. Fortunately, the worst errors occurred at the most forward angles, where the results of the previous calculations could be used. In fact, since zone 10 subtends an angle of 3.1° in Fig. 1, I was able to use the previous calculations out to 3°. The results are shown in Figs. 3-6, which give photon energy content inside the zone 10 per incident electron per steradian as a function of photon angle (averaged over 1° intervals), again using a parallel 17 MeV electron beam. The smooth curves were hand-drawn to give reasonable fits to the calculated points. The quoted half-widths at half maximum are based on the smooth curves, while the medians (i.e., the angles within which half the photons are found) come from the raw calculations.

In accordance with Refs. 1 and 3, the photon energy content per steradian at 0°, resulting from a converging electron beam, was found by adding up the total photon energy content (as given by the parallel-beam angular distribution calculation) for all the photon angular bins up to the assumed electron convergence angle, and then dividing by the appropriate solid angle. The results for the 36.75-mil target are shown in Fig. 7 as a function of convergence angle. Note that at an angle of 6°, which is the nominal value for the FXR, the forward flux is only about half what it is for a 1° angle. Note also that the flux at 0° is about 8% greater than the average value of the flux between 0 and 1°. A comparison of the results for the four targets at three different convergence angles is shown in the following table:

Thickness (mils)	Photon*MeV/electron/steradian(0°) 3 degrees	 6 degrees	 9 degrees
24.5	10.02 ± 0.20	7.81 ± 0.24	6.12 ± 0.15
36.75	10.51 ± 0.21	7.81 ± 0.23	6.14 ± 0.15
49	10.31 ± 0.21	7.74 ± 0.23	6.05 ± 0.15
61.25	10.52 ± 0.20	8.03 ± 0.23	6.23 ± 0.16

IV. DISCUSSION

In spite of all the artificialities, assumptions, and simplifications used in this study, the main conclusion seems quite clear: that the x-ray output from a tantalum target in this bullnose geometry is practically independent of target thickness. It seems unlikely that making the model used here more complicated or sophisticated would substantially alter that conclusion. However, at this point it is worth while to ask why this should be so, since one might expect naively that the x-ray production would, to lowest order, vary linearly with target thickness. In fact, examination of the SANDYL outputs shows that the total number of photons coming out of the target with energies greater than 0.75 MeV does indeed increase almost linearly with thickness; the "almost" results from the greater photon attenuation in the thicker tantalum and from the lower rate of bremsstrahlung production as the electrons slow down in the target. However, it is also true that as the thickness is increased the fraction of photons coming out of the target at large angles increases, due to the greater amount of multiple scattering of electrons in the target. Evidently, these two effects nearly cancel, and so the total number of photons that are capable of making it through the collimation system stays about the same.

There is one more effect that has to be considered. Since the electron beam still has a lot of energy when it enters the beryllium vacuum plug, it will produce some bremsstrahlung there as well as in the target, and the amount produced will be greater for thinner targets. In fact, for the 24.5-mil and 36.75-mil targets, the number of photons leaving the beryllium is greater than the number entering, although in the forward direction there is still a net attenuation. In addition, there appears to be some x-ray production in the beryllium beam stop, but it is detectable only for the 24.5-mil target. It would seem advisable, therefore, to avoid using too thin a target, since the spot size will get larger if we have an extended source of x-rays.

V. CONCLUSIONS

SANDYL calculations have been performed for the standard FXR bullnose geometry, using tantalum target thicknesses of 24.5, 36.75, 49, and 61.25 mils. I have used these calculations to determine the flux of forward-directed bremsstrahlung x-rays produced by a 17 MeV electron beam from the FXR. Although the calculations were done for a parallel beam, I was able to use them to compute the flux reduction that would result from using a more realistic converging beam with an arbitrary convergence angle.

The main conclusion to be drawn from these calculations is that the forward x-ray flux is a very weak function of target thickness. In fact, to within the statistical errors of the Monte Carlo code, the flux is independent of target thickness over the 24.5-61.25 mil range. Moreover, this conclusion is valid for any reasonable beam convergence angle. Therefore, both the 40 mil design thickness and the ±5 mil tolerance for the new target wheel are quite reasonable. Further reductions in tantalum thickness (to save money, for example) are not advisable, due to the possible increase in the spot size resulting from x-ray production in the beryllium. Increasing the thickness might indirectly improve the forward x-ray flux by reducing the amount of beryllium needed to stop the electrons, but it would also increase the activation of the bullnose structure because of the greater large-angle x-ray flux.

REFERENCES

1. D.R. Goosman, "Monte-Carlo Calculations of Forward Directed Bremsstrahlung Produced by 20 and 45 MeV Electrons", UCID 19972, December 27, 1983.

2. H.M. Colbert, "SANDYL, a Computer Program for Calculating Combined Photon-Electron Transport in Complex Systems", Sandia National Laboratories Report SLL-74-0012, 1974.
3. David R. Goosman, "Radiographic X-Ray Flux Monitoring During Explosive Experiments by Copper Activation". UCRL-93074, January 28, 1986.

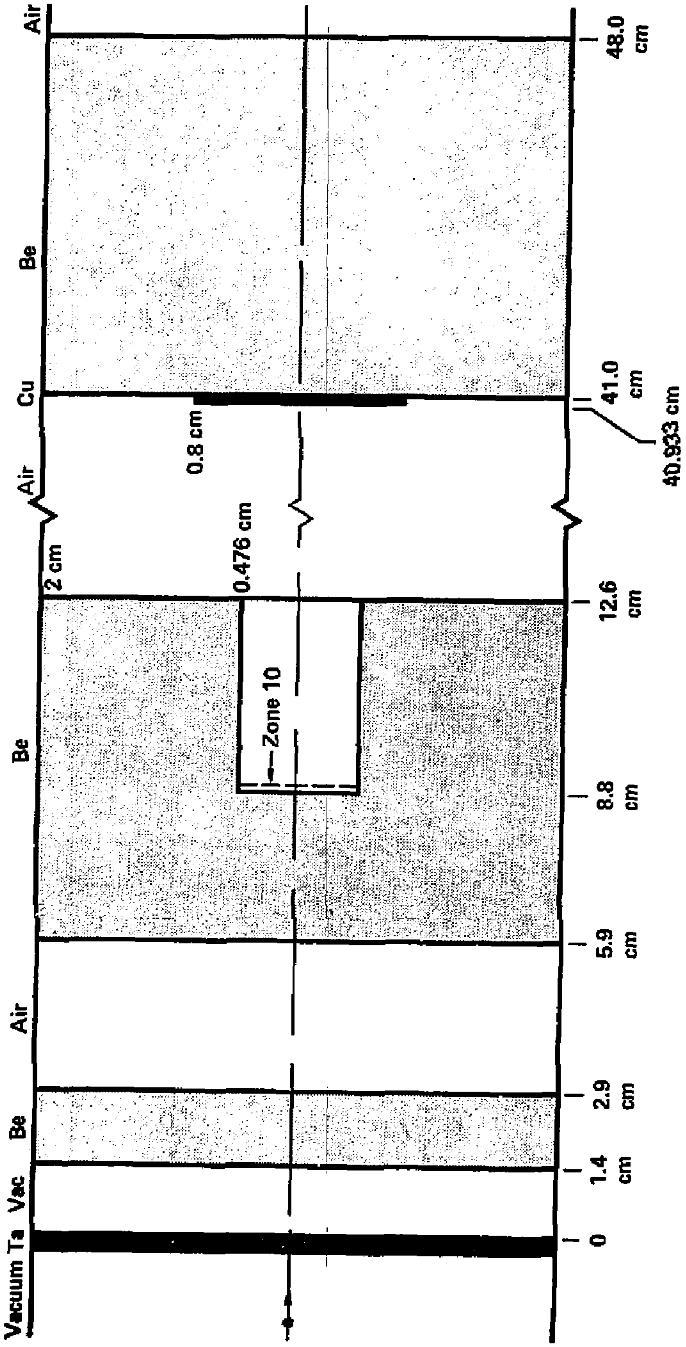
Vacuum
Ta
Vac
Be
Air
Be
Air
Cu
Be
Air
0
1.4 cm
2.9 cm
5.9 cm
8.8 cm
12.6 cm
2 cm
0.476 cm
Zone 10
0.8 cm
40.933 cm
41.0 cm
48.0 cm

Fig. 1

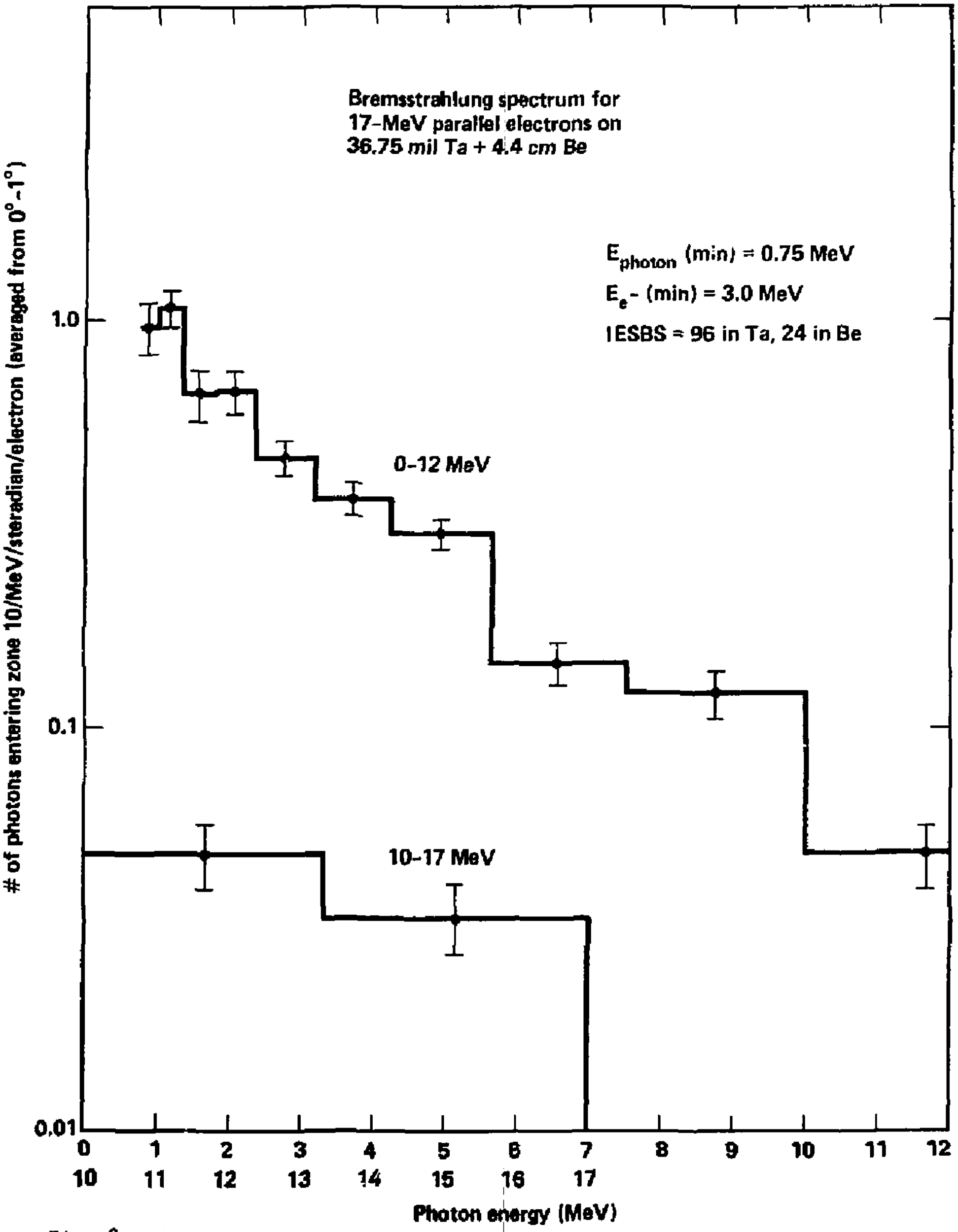
Bremsstrahlung spectrum for
17-MeV parallel electrons on
36.75 mil Ta + 4.4 cm Be
E_{photon} (min) = 0.75 MeV
E_{e^-} (min) = 3.0 MeV
IESBS = 96 in Ta, 24 in Be
0-12 MeV
10-17 MeV
# of photons entering zone 10/MeV/steradian/electron (averaged from 0°-1°)
1.0
0.1
0.01
0 1 2 3 4 5 6 7 8 9 10 11 12
10 11 12 13 14 15 16 17
Photon energy (MeV)

Fig. 2

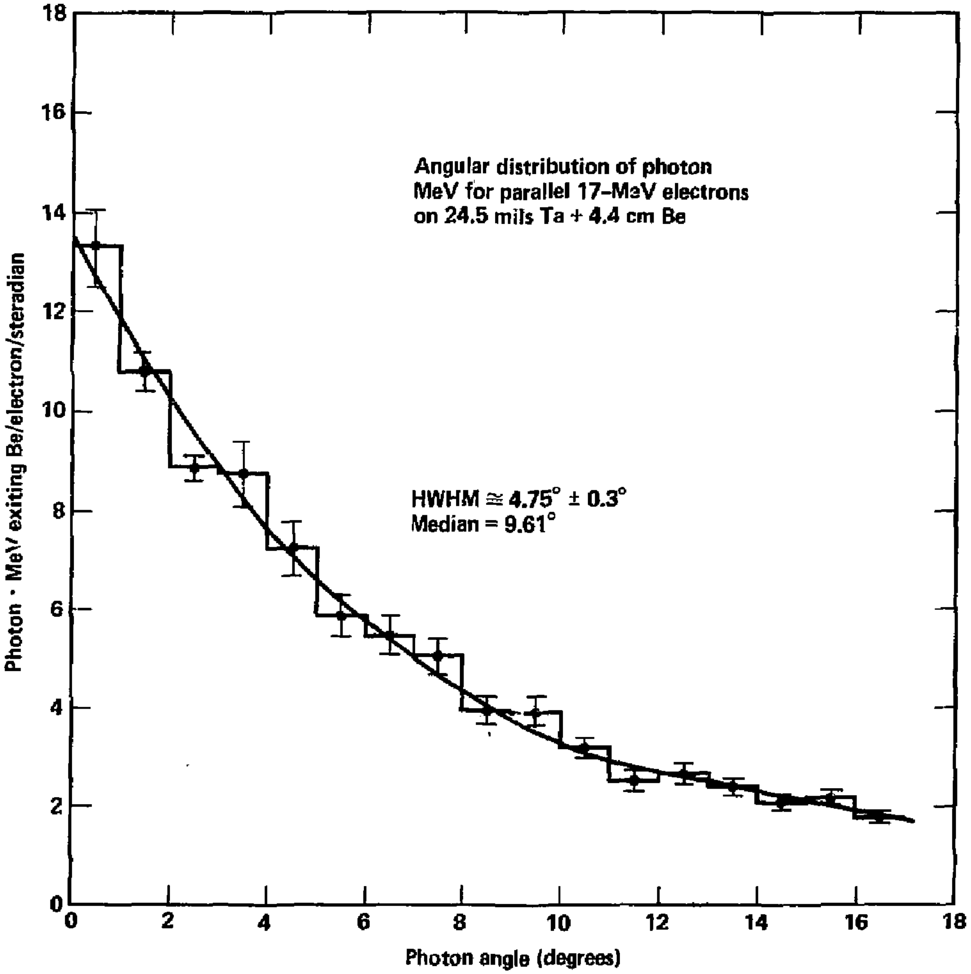
Angular distribution of photon
MeV for parallel 17-MeV electrons
on 24.5 mils Ta + 4.4 cm Be
HWHM ≅ 4.75° ± 0.3°
Median = 9.61°
Photon · MeV exiting Be/electron/steradian
Photon angle (degrees)
0
2
4
6
8
10
12
14
16
18

Fig. 3

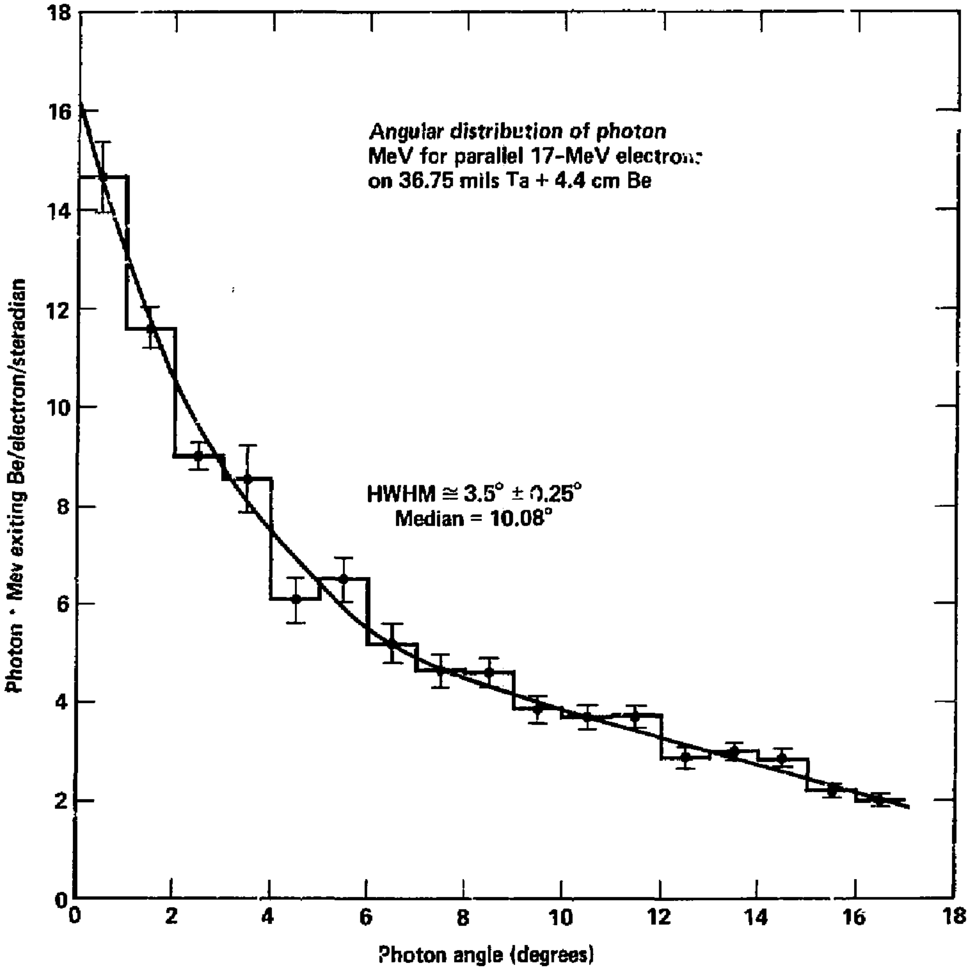
Angular distribution of photon
MeV for parallel 17-MeV electrons
on 36.75 mils Ta + 4.4 cm Be
HWHM ≅ 3.5° ± 0.25°
Median = 10.08°
Photon · Mev exiting Be/electron/steradian
Photon angle (degrees)
0
2
4
6
8
10
12
14
16
18

Fig. 4

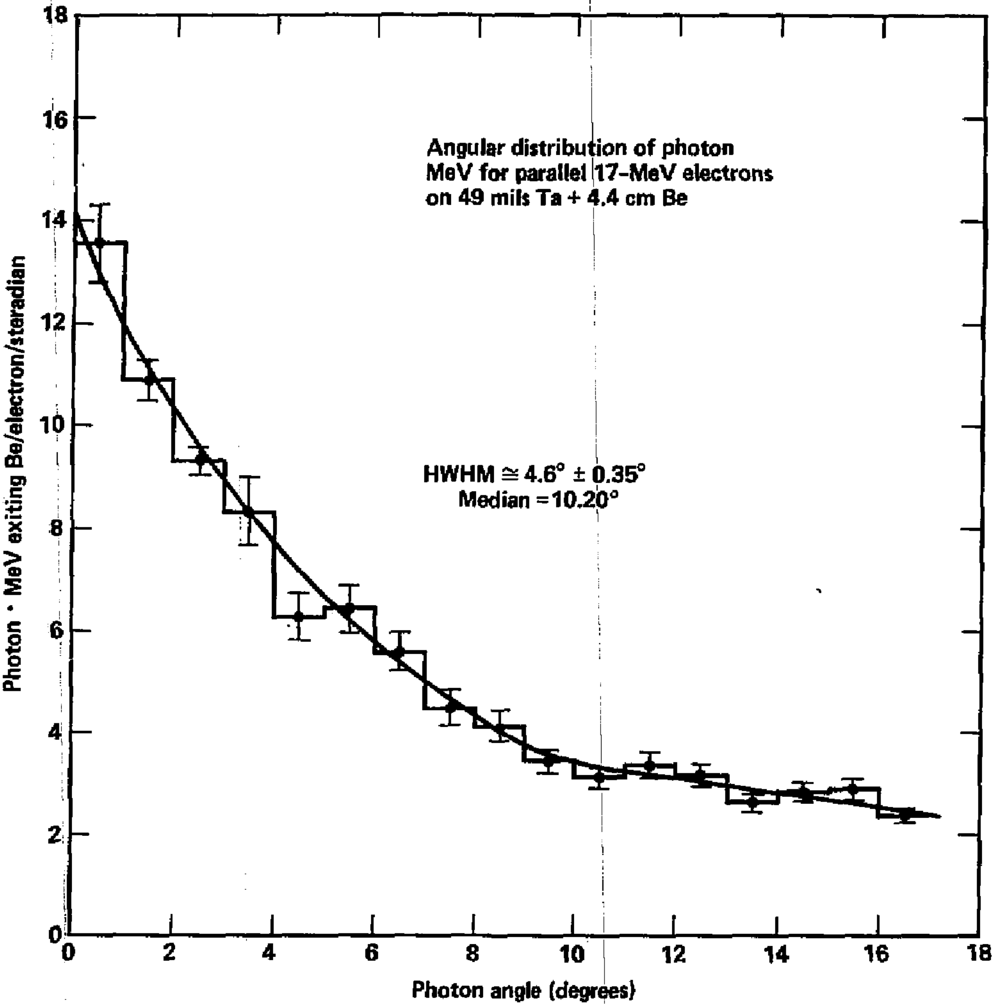
Angular distribution of photon
MeV for parallel 17-MeV electrons
on 49 mils Ta + 4.4 cm Be
HWHM ≅ 4.6° ± 0.35°
Median = 10.20°
Photon • MeV exiting Be/electron/steradian
Photon angle (degrees)
0
2
4
6
8
10
12
14
16
18

Fig. 5

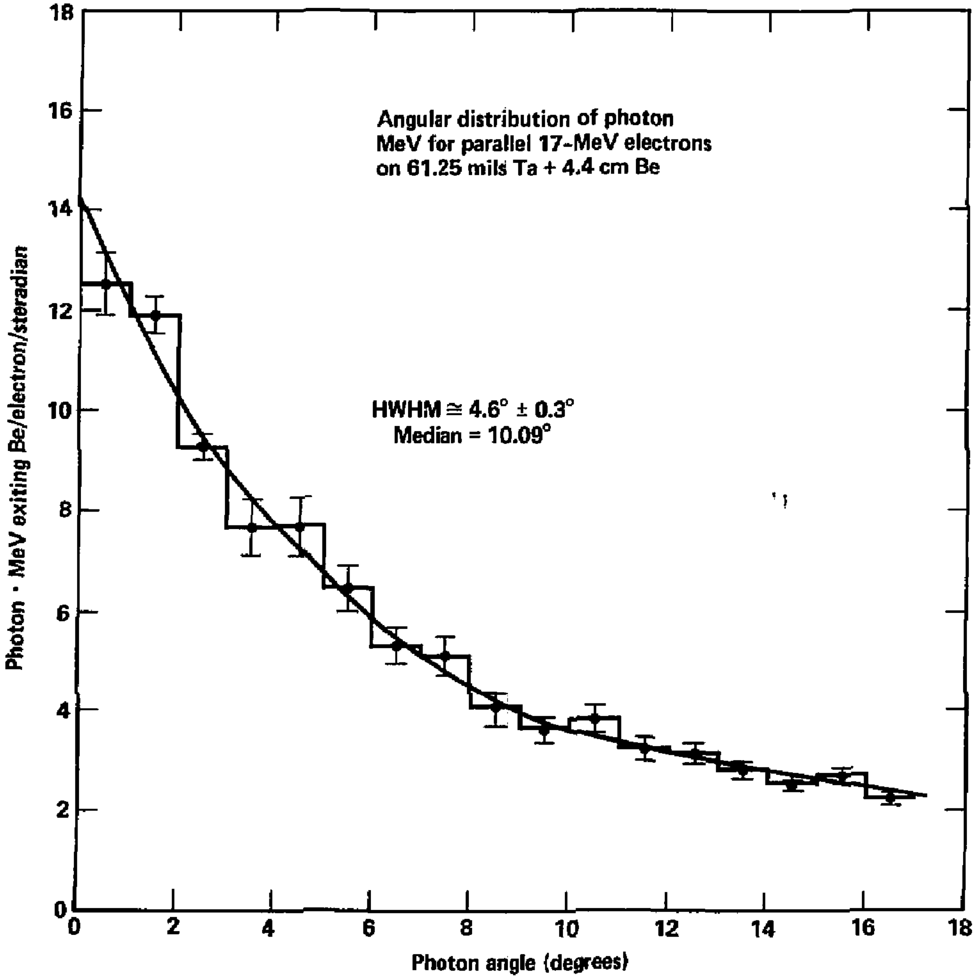
Angular distribution of photon
MeV for parallel 17-MeV electrons
on 61.25 mils Ta + 4.4 cm Be
HWHM ≅ 4.6° ± 0.3°
Median = 10.09°
Photon · MeV exiting Be/electron/steradian
Photon angle (degrees)
0
2
4
6
8
10
12
14
16
18

Fig. 6

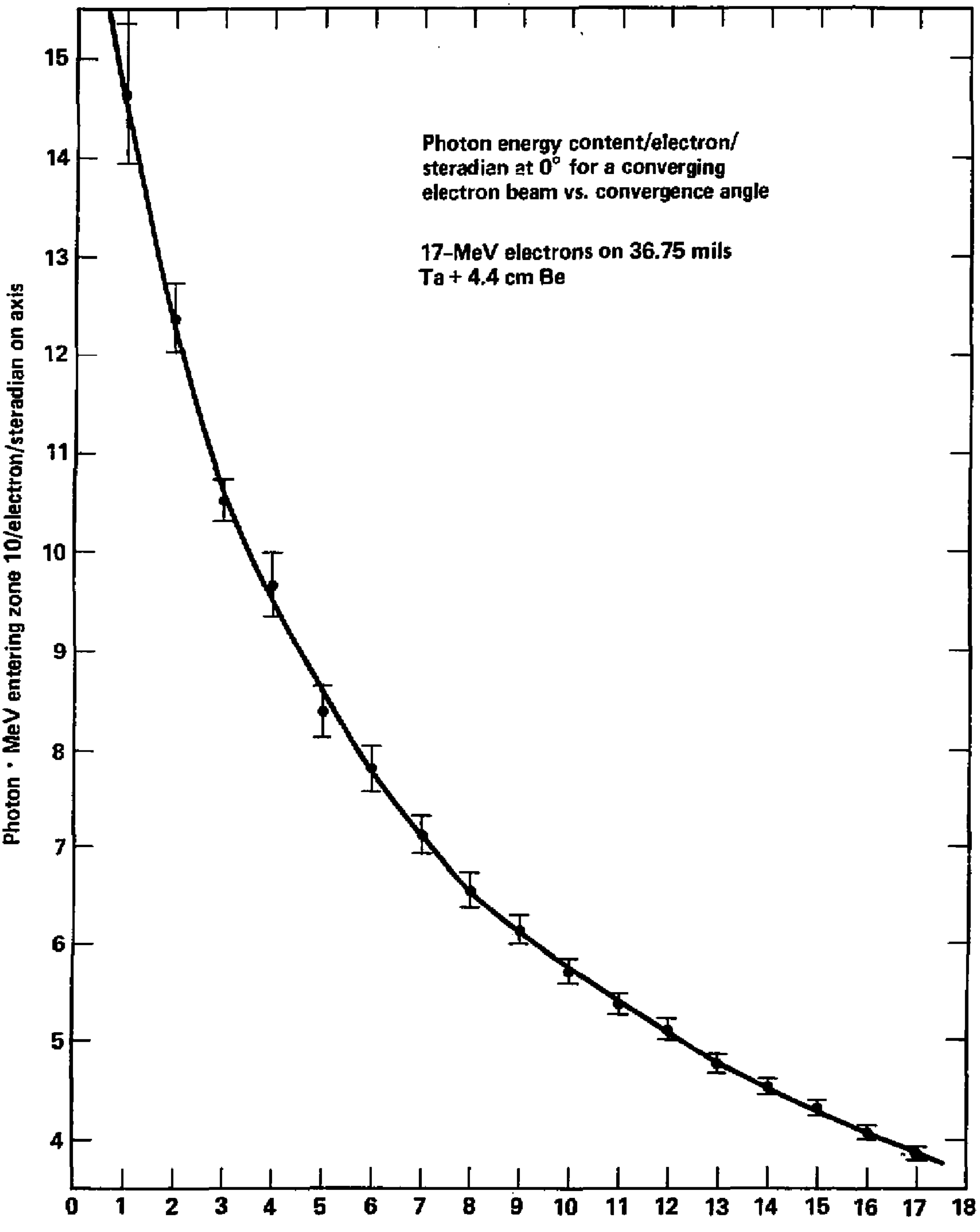
Photon energy content/electron/
steradian at 0° for a converging
electron beam vs. convergence angle
17-MeV electrons on 36.75 mils
Ta + 4.4 cm Be
Photon · MeV entering zone 10/electron/steradian on axis
θ_e^{max} = electron half-angular convergence in degrees
4
5
6
7
8
9
10
11
12
13
14
15
0
1
2
3
4
5
6
7
8
9
10
11
12
13
14
15
16
17
18

Fig. 7